New erbium-doped photonic materials

L. H. Slooff
FOM Institute for atomic and molecular physics, Kruislaan 407, P.O. Box 41883,
1009 DB Amsterdam, email: Slooff@amolf.nl

Supervisor:
Prof. dr. A. Polman

Abstract
Erbium-doped organic complexes are synthesized and show room temperature photoluminescence at 1.54 μm. The luminescence lifetimes, and temperature quenching are studied for complexes with different structures, and complexes in which specific H atoms are replaced by D atoms. Coupling of the Er^{3+} with nearby C-H and O-H bonds causes quenching of the luminescence. These erbium-doped organic complexes may be used in planar optical waveguide amplifiers operating at 1.54 μm.
Hydrogenated amorphous silicon films, deposited by plasma enhanced chemical vapour deposition are implanted with erbium ions. The 1.54 μm photoluminescence and the effect of post implantation annealing and O co-doping are studied. Erbium implanted p-i-n diodes show room temperature electroluminescence at 1.54 μm under forward bias.

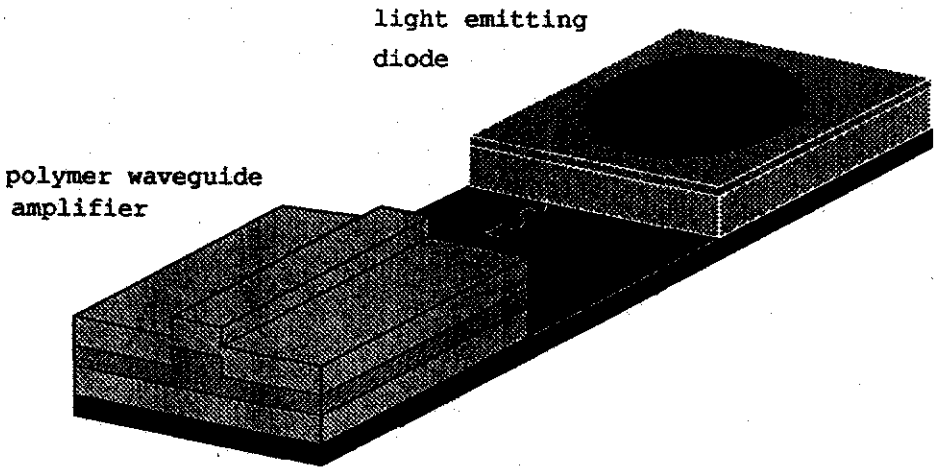

This work was performed at the FOM institute for atomic and molecular physics between September 1995 and September 1996 as part of the graduation program of the study physics at the University of Utrecht.

New erbium-doped materials

Part I: Photoluminescence of erbium-doped organic complexes

Part II: Light emitting diodes based on erbium-implanted hydrogenated amorphous silicon

Contents

Part I

Photoluminescence of erbium-doped organic complexes

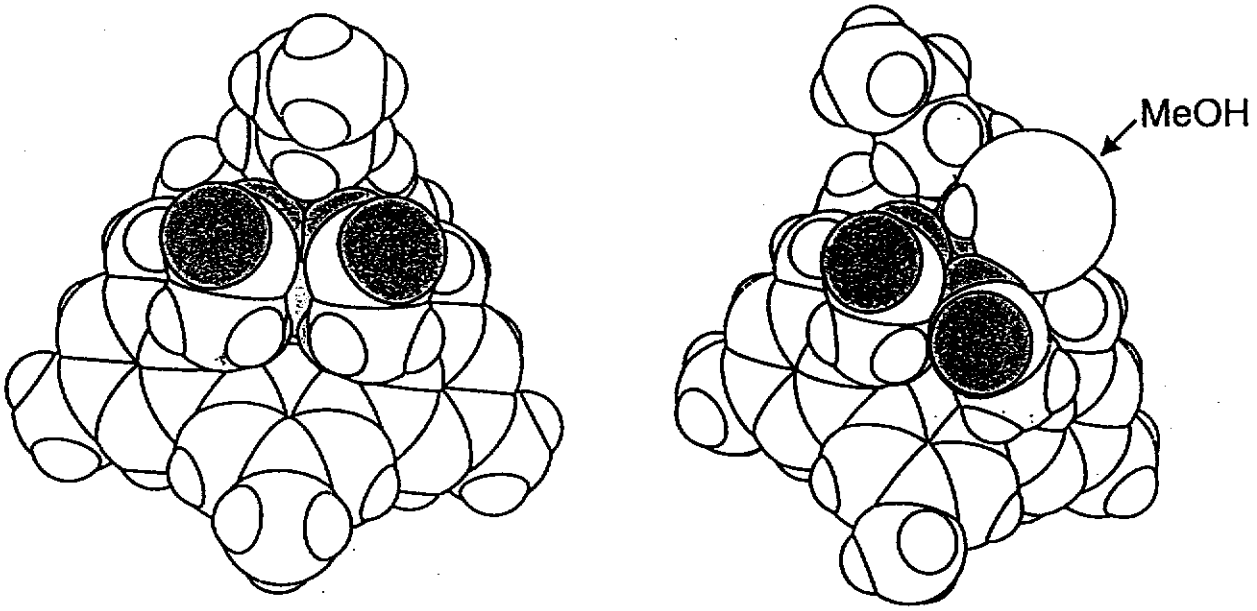

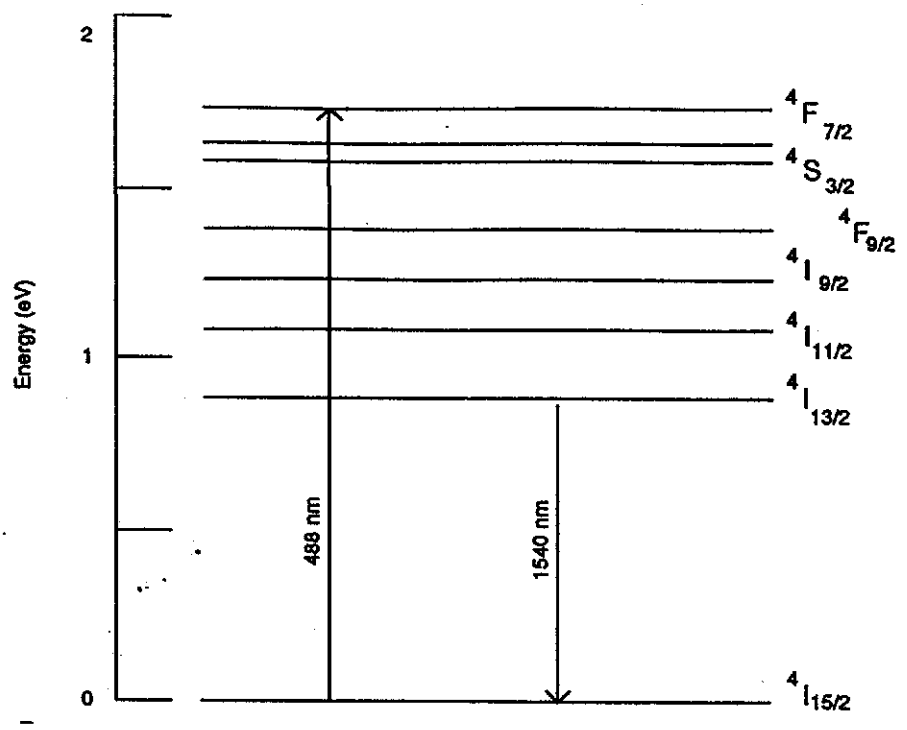

Fig. 1. Schematic energy diagram of the Er^{3+} ion. Shown are the excitation band $^4F_{7/2}$ and the transition from the first excited state $^4I_{13/2}$ to the ground state $^4I_{15/2}$.

1. Introduction

Erbium (Er) doped materials have become a major research topic because of their potential use in optoelectronic devices and systems [1-3]. In its trivalent state the Er^{3+} ion shows an intra 4*f*-shell transition from the first excited state ($^4I_{13/2}$) to the ground state ($^4I_{15/2}$) (see figure 1), which occurs at a wavelength of 1.54 μm. In the free Er^{3+} ion optical intra 4*f*-shell transitions are parity forbidden. Incorporation of Er^{3+} in a solid host induces mixing of states of opposite parity which makes some of the transitions allowed. These transitions are rather sharp due to the fact that the partially filled 4*f*-shell is shielded by filled 5*s* and 5*p* shells. The lifetime of the first excited state can be as long as several milliseconds. The sharp and temperature independent emission and the long luminescence lifetimes make Er-doped materials ideally suited for the fabrication of lasers and optical amplifiers operating at 1.54 μm, a standard telecommunication wavelength. Indeed Er-doped silica fibers are nowadays being used as optical amplifiers in long distance optical fiber links [4,5].

Recently, interest has also focused on Er-doped planar optical waveguides. Net optical gain has been demonstrated in Er-doped silica and Al_2O_3 waveguides on a planar substrate [6-10,11].

Polymer waveguides are becoming more and more important, both as fibers and in thin film configurations. A variety of optical components based on planar polymer waveguides (splitters, switches, multiplexers) have been made [12]. It is therefore interesting to study the doping of polymers with Er ions, and to investigate if optical amplifiers could be achieved in Er-doped planar polymer waveguides
Rare-earth ions can not be dispersed directly in an organic matrix . One way around this problem is to first incorporate the Er^{3+} ions in a complex which can then be dispersed in a polymer film. The complex has to be designed such that it provides enough co-ordination sites to bind the Er^{3+} ion.

In this paper we study the optical properties of Er-doped polydentate hemispherands. Three COO^- groups are bound to the Er^{3+} ion, forming an overall neutral complex. The Er ion is encapsulated in a cage like ligand configuration. In this way the Er ion may be shielded from e.g. OH impurities in the solvent which are known to quench the luminescence due to coupling to vibrational modes of the OH bond [13,14]. A polymer-like tail makes the complex soluble in a polymer matrix. The coupling of the Er^{3+} ion to vibrational modes of nearby O-H and C-H bonds is studied by selective deuteration experiments, and the effect of changing the complex structure is also investigated. It is found that the Er^{3+}-complexes show clear room temperature emission at 1.54 μm with a lifetime in the range of <5-110 μs, corresponding to a quantum efficiency of roughly 10^{-1} - 10^{-3}. Finally a performance estimate for a planar optical amplifier based on these Er-doped complexes is made.

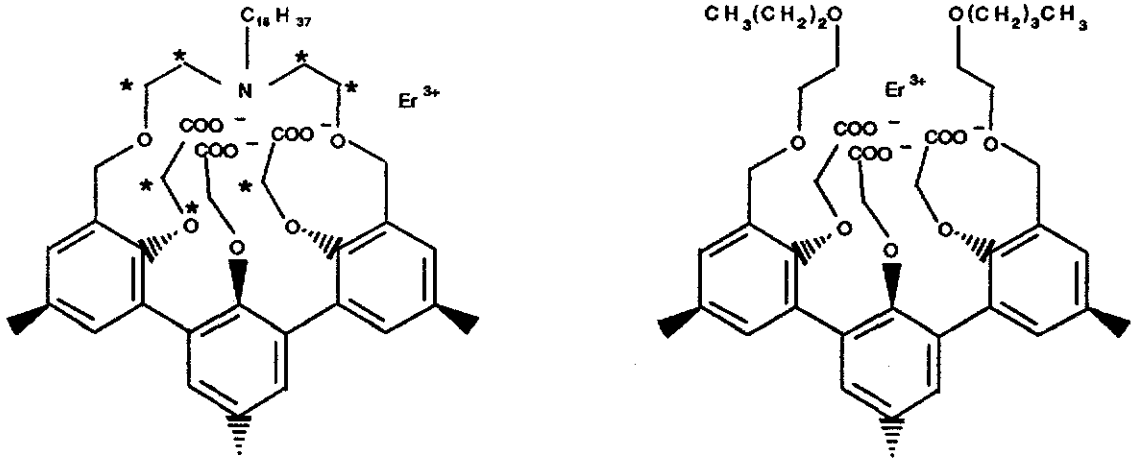

cyc-H: cyclic Er^{3+}-complex; 2 H atoms at ✱
cyc-D: deuterated cyclic Er^{3+}-complex; 2 D atoms at ✱

acyc-H: acyclic Er^{3+}-complex

Fig. 2. Schematic representation of the structures of the Er^{3+}-complexes. The outer two benzene rings lie in one plane which is tilted backwards, whereas the middle benzene ring is tilted forwards. In this way a cage is constructed encapsulating the Er^{3+} ion.

2. Experimental

Three different Er^{3+}-complexes were prepared in a multi-step synthesis procedure, described in ref. [15]. Figure 2 shows a schematic picture of the cyclic Er^{3+}-complex (cyc-H), the deuterated cyclic Er^{3+}-complex (cyc-D) and the acyclic Er^{3+}-complex (acyc-H). The structure of the two cyclic complexes is identical, but in the case of cyc-D the H atoms nearest to the Er ion are replaced by D atoms (see ✶ in figure 2). A slightly different structure is obtained for the acyclic complex (acyc-H) where the polymer-like tail at the top of the complex consists of two $O(CH_2)_nCH_3$ strings (with n=2,3) instead of one $C_{18}H_{37}$ string. After synthesis the Er^{3+}-complex solutions were dried, mixed with KBr and then pressed in 1.2 cm diameter tablets, or solved in deuterated butanol. KBr tablets were made with Er-doped complexes at three different Er concentrations: 0.04 at.%, 0.15 at.% or 0.26 at.% (0.1 wt.%, 0.5 wt.% or 1.0 wt.%). These concentrations do not take into account the amount of water which remains in the tablets as a result of the preparation process. The concentration of Er in the deuterated butanol solutions was: 0.12 at.% (0.19 wt.%) for cyc-H and cyc-D and 0.07 at.% (0.12 wt.%) for acyc-H.

Photoluminescence (PL) measurements were performed using the 488 nm line of an Ar ion laser at a power of 100 mW. The laser beam was modulated with a mechanical chopper at a frequency of 40 Hz or using an acousto-optic modulator at a frequency of 20 Hz. The samples were mounted in a closed-cycle helium cryostat, enabling measurements at temperatures ranging from 12 K to room temperature. The KBr tablets were first mounted onto a piece of crystalline silicon (c-Si). The deuterated butanol solutions were measured in a cuvet which was connected to the cooled sampleholder with silverpaint, ensuring good thermal contact. The PL signal was focused into a monochromator and detected with a liquid-nitrogen-cooled Ge detector, using standard lock-in techniques. The spectral resolution was 6 nm. Lifetime measurements were performed by monitoring the luminescence decay after switching off the pump beam using the acousto optic modulator. The time resolution ranged from 1.5 μs to about 10 μs. Some lifetime measurements were made using a 1.48 - 1.58 μm bandpass filter, replacing the monochromator. The decay curves were averaged using a digitising oscilloscope.

Reflection (R) and transmission (T) measurements were performed using a Perkin Elmer Lambda 2S Spectrometer which measures the reflected and transmitted intensities by an integrating sphere. The spectral resolution was 0.3 nm. The extinction cross section C_{ext} is derived from R and T using the following formula (see ref. [16]):

$$T = \frac{(1-R)^2 e^{-\alpha h}}{1-R^2 e^{-2\alpha h}} \tag{1}$$

where h is the thickness of the sample and $\alpha = C_{ext} * N$ is the attenuation coefficient with N the number of Er atoms per cm^3. This results in:

$$C_{ext} = -\ln\left(\frac{(1-R)^2 - \sqrt{(1-R)^4 + 4T^2R^2}}{-2TR^2}\right)\frac{1}{hN} \tag{2}$$

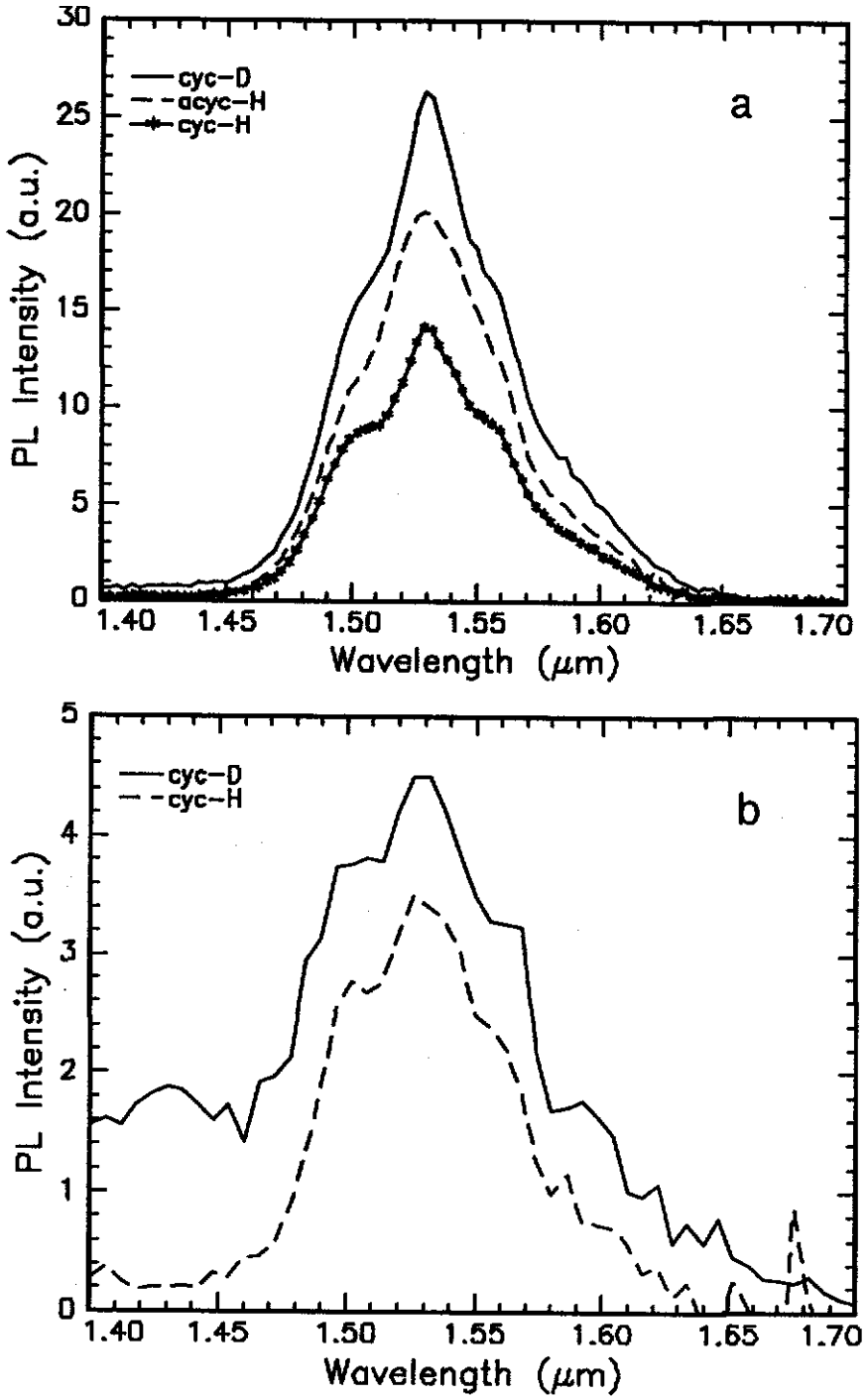

Fig.3. Room temperature PL spectra of Er^{3+}-complexes in a) KBr tablets (power 100 mW) and in b) deuterated butanol (power 140 mW) at a pump wavelength of 488 nm.

3. Results and discussion

3.1 Photoluminescence excitation and emission spectroscopy

Figure 3(a) shows room temperature PL spectra for the three complexes in KBr. The peak around 1.54 μm is typical for Er^{3+} luminescence and is due to the transition from the first excited state to the ground state (see figure 1). The full width at half maximum (FWHM) of all spectra is 70 nm. This is much wider than for Er-implanted SiO_2 (11 nm FWHM), phosposilicate glass (25 nm FWHM) (see ref. [17]), sodalime silicate glass (19 nm FWHM see ref. [18]) and Al_2O_3 (55 nm FWHM see ref. [19]). This enables a wide gain bandwidth for optical amplification. As can be seen, the shape of the spectra for the different complexes is more or less the same, indicating that the direct environment of the Er^{3+} ion is the same in these complexes. As the Er^{3+}-complexes in KBr all have a concentration of 1.0 wt.%, it is possible to compare the PL intensities of these samples The uncertainty in the measured PL intensity is approximately 10 %, due to intensity variation across the sample. The deuterated cyclic complex (cyc-D) shows 1.8 ± 0.2 times more room temperature PL intensity than the cyc-H complex. The acyclic complex has 1.4 ± 0.2 times more intensity than the cyclic complex.

Measurements of the cyclic complexes in deuterated butanol solution are shown in figure 3(b). Although the pump power for these measurements was higher than those for figure 3(a) (140 mW vs. 100 mW), the relative intensities are much lower than those for the KBr samples in figure 3(a), which is attributed to the lower Er density in the solution. Because the cyc-H and cyc-D complexes did not completely dissolve, the measurements were performed on the solution above the precipitate. As the concentration of the Er^{3+}-complexes in the solution is not exactly known, the PL intensities in figure 3(b) can not be directly compared. The PL spectra for the complexes in deuterated butanol are peaked at 1.54 μm, with a FWHM of 60 nm, similar to the data in figure 3(a). The intensity of acyc-H in the solution was too low to be measured.

Extinction spectra of acyc-H, cyc-H and cyc-D in KBr are shown in figure 4. The absorption lines of the Er^{3+} are clearly seen and are indicated in the figure, together with the level notation. The strong background signals in the range up to 600 nm are attributed to light scattering that is not detected in the reflection and transmission measurement. Different amounts of scattering in the samples results in a different background.

Subtracting the background and taking into account the exact Er areal density for these samples (acyc-H $8.54*10^{18}$ /cm^2 , cyc-H $8.21*10^{18}$ /cm^2), the absorption cross sections for the $^4I_{15/2} \rightarrow {}^4F_{7/2}$ transition can be derived: $(2.3 \pm 0.5)*10^{-20}$ cm^2 for acyc-H and $(1.4 \pm 0.3)*10^{-20}$ cm^2 for cyc-H. These absorption cross sections are 2 to 3 times higher than the cross sections for Er-doped glasses ([20,21]), and for Er-implanted Al_2O_3 [22]. This may be related to differences in average electron distribution around the Er for organic complexes compared to anorganic hosts.

The 1.6 times higher absorption cross section for acyc-H compared to cyc-H can thus explain the 1.4 ± 0.2 times higher PL intensity found for acyc-H in figure 3(a).

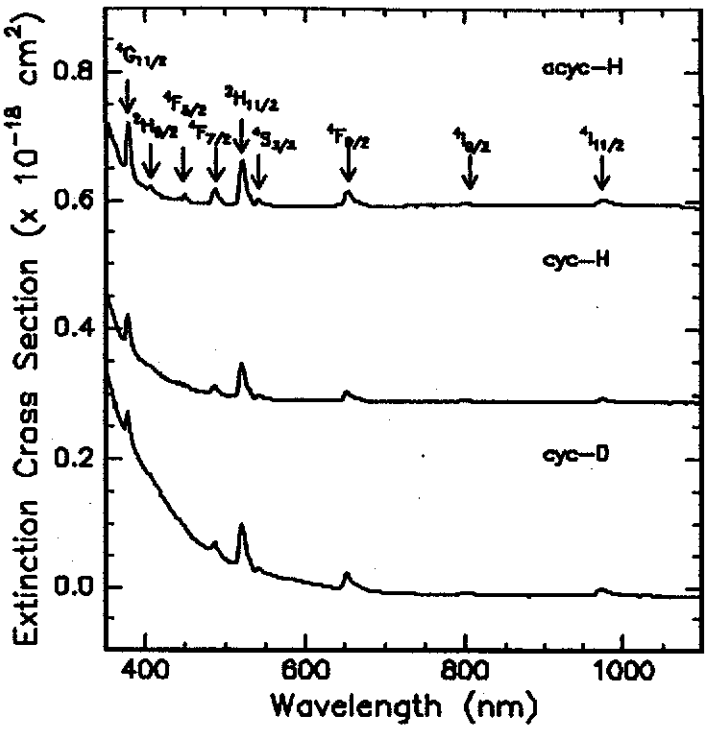

Fig. 4. Extinction spectra of acyc-H, cyc-H and cyc-D in KBr. The data for cyc-H and acyc-H are shifted by 0.3 and 0.6 for clarity.

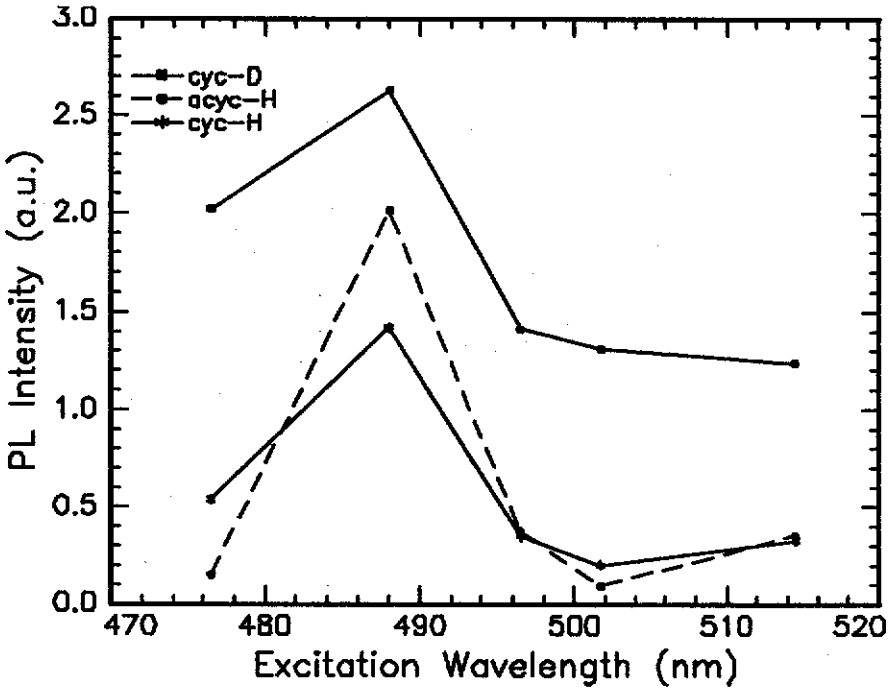

Fig. 5. Room temperature excitation spectrum of Er^{3+}-complexes in KBr; 1.0 wt. % in KBr (1.0 wt.%). The 1.54 μm PL intensity is measured as a function of excitation wavelength at a fixed pump power of 100 mW.

The $^4I_{15/2} \rightarrow {}^4F_{7/2}$ absorption cross section of cyc-D, which is $(1.6 \pm 2)*10^{-20}$ cm^2, is about the same as for cyc-H and thus the 1.8 ± 0.2 fold higher PL intensity for cyc-D compared to cyc-H may be attributed to a difference in the non-radiative decay of the first excited state of the Er^{3+} ion. As cyc-H has C-H bonds in the first co-ordination sphere around the Er^{3+} ion, non-radiative decay via higher order C-H vibrations (E_0 = 2960 cm^{-1}) can depopulate the first excited state of the Er^{3+} ion (E = 6500 cm^{-1}) resulting in less PL intensity. This quenching mechanism is also seen in research on Eu^{3+}-complexes (see ref. [15]). The deuterated complex would then show less quenching due to the lower vibration energy of C-D.

The extinction spectra of figure 4 also show that more luminescence is to be expected upon pumping at 520 nm, as the absorption peak of the Er is about 3 times higher. As this is not an Ar laser wavelength, in the present experiments 488 nm was chosen for pumping the Er^{3+} ion. The absorption cross section σ_a is directly related to the emission cross section σ_e according to [23]:

$$g_1 \int \nu^2 \sigma_a(\nu) d\nu = g_2 \int \nu^2 \sigma_e(\nu) d\nu \qquad (3)$$

where g_i is the degeneracy of level i and ν is the photon frequency. This means that a higher absorption cross section results in a higher emission cross section. As the radiative lifetime τ is given by:

$$\frac{1}{\tau} = \frac{8\pi n^2}{c^2} \int \nu^2 \sigma_e(\nu) d\nu \qquad (4)$$

with n the refractive index, and c the speed of light, the higher absorption cross section corresponds to a lower radiative lifetime. At this stage it is not possible to determine the purely radiative decay rate of the Er-doped complexes, but due to the relative high cross sections it is expected to be significant lower than for Er-doped anorganic materials such as Al_2O_3 and SiO_2 (a rough estimate would be τ_{rad} = 1 ms.

Figure 5 shows photoluminescence excitation spectra, taken by measuring the PL intensity at 1.54 μm, for different wavelengths of the Ar ion laser : 476.5 nm, 488 nm, 496.5 nm, 501.4 nm and 514.5 nm, at a constant pump power of 100 mW. Data are shown for all three complexes in KBr, at an Er concentration of 1.0 wt. %. This figure shows that within the 470-514 nm wavelength range, the most efficient excitation wavelength is roughly 488 nm. All three complexes show the same trend.

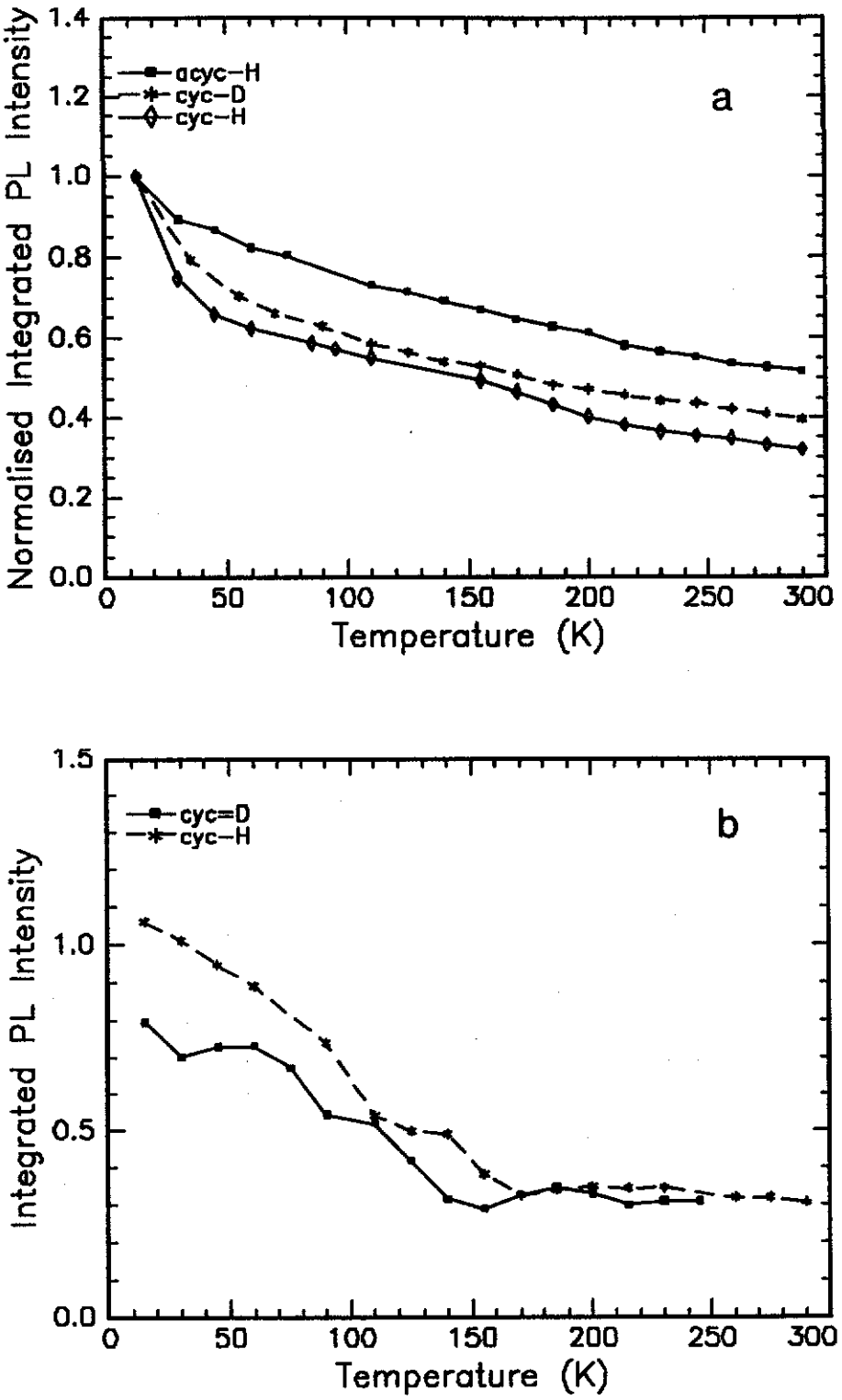

Fig.6. Temperature dependence of the integrated PL intensity of Er^{3+}-complexes in a) KBr and b) deuterated butanol solution.

3.2 Photoluminescence quenching and lifetime measurements

Figure 6(a) shows measurements of the integrated 1.54 μm PL intensity, normalised to the intensity at 15 K, between 15 and 300 K for the three complexes in KBr. Cyc-H and cyc-D show the same trend as function of temperature, with a quenching by a factor 3 between 15 K and room temperature. Acyc-H shows a temperature quenching of a factor 2 in the same temperature range. Figure 6(b) shows similar measurements for cyc-H and cyc-D in deuterated butanol. The PL intensity of acyc-H was too low to measure the temperature quenching. It seems as if the integrated PL intensity for cyc-H and cyc-D is more or less constant at higher temperature (>170K). This behaviour is slightly different than that seen for the KBr tablets.

Figure 7 shows luminescence decay measurements at 1.54 μm for acyc-H and cyc-D in the deuterated butanol solution measured at 15 K. In all measurements the signal intensities are low, resulting in a bad signal to noise ratio. A single exponential fit through the data results in a lifetime of 110 μs for acyc-H and < 12 μs for cyc-D. The lifetime for cyc-H (not shown) is also < 12 μs.

Luminescence decay measurements for the complexes in KBr (not shown) all result in lifetimes < 5 μs. Table 1 lists all measured lifetimes.

	τ in butanol solution (μs)	τ in KBr tablet (μs)
acyc-H	110	<5
cyc-H	<12	<5
cyc-D	<12	<5

Table 1: Luminescence lifetimes τ of the Er^{3+}-complexes at 15 K.

The PL intensities for the complexes in KBr are similar to those for Er-doped SiO_2 thin films (data not shown). As the total Er areal density in the KBr tablets ($8 * 10^{18}$ Er/cm^2) is much higher than in the SiO_2 films ($6 * 10^{15}$ Er/cm^2), this suggests that significant luminescence quenching takes place in the organic complexes. Indeed the measured luminescence lifetimes are much shorter than the expected spontaneous emission lifetimes on the order of 1 ms (see section 3.1). Figure 6 shows that this quenching process is almost temperature independent.

One possible quenching mechanism is the presence of OH at the complexes. OH is a constituent of the liquids used in the preparation process of the Er^{3+}-complexes , see ref. [15], so it is possible that an OH molecule remains bound at the complex. An OH molecule positioned near the Er^{3+} ion can result in quenching of the luminescence, because the second order vibrational energy ($E_0 = 3680$ cm^{-1}) is resonant with the Er transition ($E = 6500$ cm^{-1}). If such a quenching is strong, substitution of C-H by C-D bonds will have only a very small effect on the temperature quenching (as is seen in figure 6). Solving the complexes in deuterated butanol results in a slightly different quenching behaviour as seen in figure 6(b). While the PL intensity of the complexes in KBr is continuously decreasing upon increasing the temperature, in deuterated butanol the PL intensity is more or less constant above 170 K. This might be connected with the fact that the freezing point of butanol is 187 K. Below this temperature the samples are frozen and show cracks.

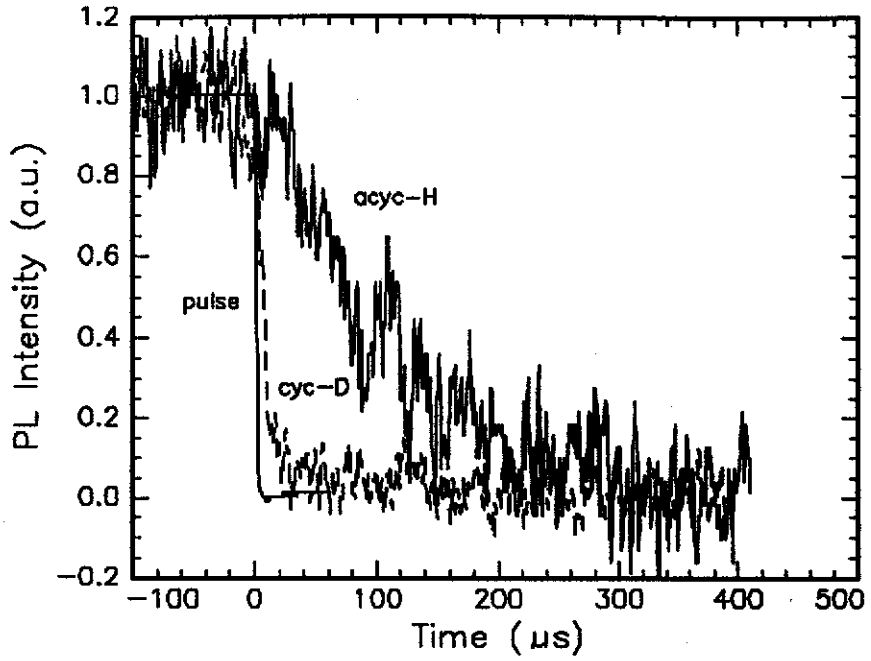

Fig.7. Photoluminescence decay at 1.54 μm, measured at 15 K for cyc-D and cyc-H in a deuterated butanol solution, shown together with the pulse trace

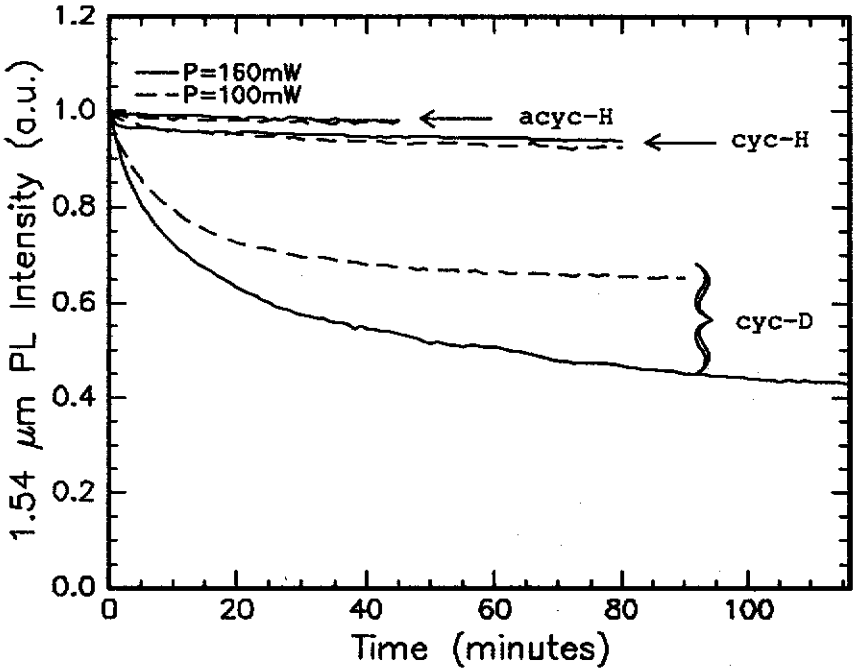

Fig 8. Temperature dependence of the 1.54 μm PL intensity of the three Er^{3+}-complexes in KBr (1.0 wt.%) measured at room temperature at 100 mW (dashed line) and 160 mW (solid line) pump power.

This also makes it hard to compare the data below the transition point, as laser scattering, and thus absorption, becomes temperature dependent.

In solution, cyc-D and cyc-H both show lifetimes $\tau < 12$ μs, while acyc-H shows $\tau = 110$ μs. The difference may be due to a difference in the COO^- branch geometry for cyclic and acyclic complexes. Molecular dynamics simulation have shown that the presence of the $C_{18}H_{37}$ polymer tail in the cyclic complex leads to a slightly smaller average distance between the Er^{3+} and the COO^- branches in these complexes than in the acyclic complexes. As a result the quenching by coupling to nearby C-H bonds may be more pronounced in the cyclic than in the acyclic complexes.

The difference in lifetime for cyclic and acyclic complexes is not observed in the KBr tablets, for which much shorter lifetimes were found (< 5 μs) for both cyclic and acyclic complexes. In this case an additional much stronger quenching process (presumably due to OH, see above) dominates the decay.

Another possible explanation for the shorter lifetimes of the Er^{3+}-complexes dissolved in KBr compared to those in the deuterated butanol solution may be the difference in Er concentration between the KBr tablets and the solutions. At high concentrations a concentration quenching effect in which the Er excitation migrates from one ion to the other, until a quenching center is met, may lower the lifetime. More systematic studies of the dependence of the PL lifetime and intensity on the Er concentration are necessary to study this in more detail. It may also be that the KBr itself affects the lifetime.

3.3 Photoluminescence degradation

Finally, figure 8 shows the time dependence of the 1.54 μm PL intensity for the three complexes in KBr at pump powers of 100 mW and 160 mW. The decrease in PL intensity is most pronounced for cyc-D. In this case the intensity dropped almost 60 % in about 1.5 hours at a pump power of 160 mW. For cyc-H and acyc-H the intensity dropped by 8% and 3% respectively.

Extinction spectra before and after laser irradiation for an hour show no differences in absorption peak at 488 nm, therefore the decrease in PL intensity is not caused by a change in absorption cross section. It may be that the irradiation causes structural changes in the complex which causes more radiative decay. More experiments are required to study this effect in more detail. It should be noted that this time dependent effect has also affected the temperature quenching measurements in figure 6. In these measurements the temperature was increased from 15 K to room temperature and hence part of the temperature quenching in figure 6 is due to this degradation effect.

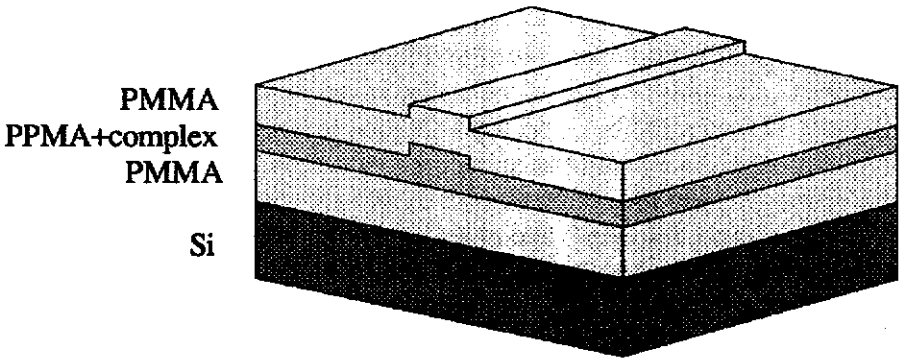

Fig. 9. Typical polymer channel waveguide structure, where a high refractive index (n = 1.57) PPMA polymer, doped with organic Er-complexes, is embedde in a low index (n = 1.49) PMMA polymer on top of a silicon substrate.

N_0	$9.04*10^{19}/cm^3$
τ	5 μs
σ_a	$1.6*10^{-20}$ cm^2
waveguide cross section	2x1 μm^2

Table 2. Parameters used for the calculations of optical gain in an Er-doped complex polymer waveguide.

3.4 Optical amplifier gain calculations

With the coefficients determined in the previous paragraphs, an estimate of the minimum pump power can be made for a planar optical amplifier based on Er-doped organic complexes. In such a polymer channel waveguide a high refractive index polymer (e.g. polyphenyl methacrylate (PPMA, n = 1.57) is embedded in a low index polymer (e.g. poly(methylmethacrylate) (PMMA, n = 1.49) (see figure 9). The waveguide is then doped with organic Er-complexes to a certain concentration. The typical waveguide dimension is 2x1 μm^2. The calculations do not take into account upconversion effects, which will increase the pump power needed for amplification (see ref. [24]). Assuming that the population of the $^4F_{7/2}$ state (see figure 1) decays rapidly to the first excited state, the population of the $4_{F7/2}$ state can be neglected. As a result, the rate at which the first excited state is populated R_{12} is equal to the pump rate of the $^4F_{7/2}$ state. The rate equations of this system then become:

$$\frac{dN_1}{dt} = -N_1 R_{12} + \frac{N_2}{\tau_2} \tag{5}$$

$$\frac{dN_2}{dt} = N_1 R_{12} - \frac{N_2}{\tau_2} \tag{6}$$

where N_1 and N_2 are the populations of the ground state and the first excited state, τ_2 is the luminescence lifetime of the first excited state, and $R_{12} = \sigma_{abs} * I/h\nu$, with I the pump intensity, σ_{abs} is the pump absorption cross section and $h\nu$ the pump photon energy. Under steady state conditions the populations of the ground state and first excited state are:

$$N_1 = \frac{\frac{1}{\tau_2}}{\frac{1}{\tau_2} + R_{12}} N_0 \tag{7}$$

$$N_2 = \frac{R_{12}}{\frac{1}{\tau_2} + R_{12}} N_0 \tag{8}$$

where N_0 is the total Er concentration. The optical gain is given by σ_{abs} (N_2-N_1) times the fraction of light which is confined in the core of the waveguide. This fraction is assumed to be 40 %.

Using the absorption cross section for cyc-D (which showed the highest room temperature PL) and a lifetime of 5 µs, net optical gain is obtained at a minimum pump power of 100 mW. The parameters used are given in table 2.

The 100 mW pump power is higher than the pump powers needed for net optical amplification in Er-doped glass amplifiers [6,7], which is mainly due to the short lifetimes. The maximum achievable optical gain in this polymer waveguide is 5.7 dB (pump power 1W). It could be increased by increasing the Er-complex concentration in the waveguides.

To improve the waveguide performance, more research has to be done on increasing the radiative lifetime and decreasing the waveguide dimensions. Another possibility is pumping at a wavelength of 275 nm. At this wavelength the complex itself can be excited very efficiently compared to direct absorption by the Er^{3+} ion at 488 nm. If energy transfer from the complex to the Er^{3+} ion is efficient, this may lead to a much lower pump power (e.g. < 1mW) needed for amplification.

4. Conclusions

Er-doped organic complexes, dissolved in KBr show clear 1.54 μm room temperature PL due to the $^4I_{13/2} \rightarrow {}^4I_{15/2}$ transition in Er^{3+}. The same complexes in a deuterated butanol solution show very little PL, which is a result of the fact that the Er concentration in these samples is lower. PL lifetimes are < 5 μs for the complexes in KBr, < 12 μs for the cyclic complexes in butanol solution, and 110 μs for the acyclic complex in the butanol solution. The $^4I_{13/2} \rightarrow {}^4I_{15/2}$ cross section is determined and ranges from $4*10^{-20}$ cm^2 to $2.3*10^{-20}$ cm^2.

From comparison to data on Er-doped anorganic hosts it is concluded that the radiative lifetime in the Er-doped organic complexes is around 1 ms. This is much higher than the measured lifetimes, and indicates that a strong quenching centre is coupled to the Er ion. This may be an OH group from the synthesis procedure, which remains attached to the complex. Deuteration of part of the complex increases the PL intensity, indicating that C-H bonds also play a role in the quenching.

Finally an optical gain calculation for a polymer channel waveguide is performed. It shows that net optical amplification at 1.54 μm may be achieved at a 488 nm pump power of 100 mW, which is rather high due to the short luminescence lifetimes of the complexes. Further optimisation of the organic synthesis procedure is required to increase the lifetime. By direct excitation of the complex via one of the aromatic rings, the pump powers for net optical gain may be reduced below 1 mW.

5. REFERENCES

[1] E. Desurvire, Sci. Am. **266**, 96 (1992).

[2] A. M. Glass, Phys. Today **46**, 34 (1993).

[3] E. Desurvire, Phys. Today **47**, 20 (1994).

[4] E. Desurvire, J. R. Simpson, and P. C. Becker, Opt. Lett. **12**, 888 (1987).

[5] R. J. Mears, L. Reekie, I. M. Jauncey, and D. N. Payne, Electron. Lett. **23**, 1026 (1989).

[6] J. Shmulovich, Y. H. Wong, G. Nykolak, P. C. Becker, R. Adar, A. J. Bruce, D. J. Muehlner, G. Adams, and M. Fishteyn, OSA Optical Amplifier Meeting, 1993, PD18-1.

[7] T. Kitagawa, K. Hattori, K. Shuto, M. Yasu, M. Kobayashi, and. M. Horiguchi, Tech. Dig. Topical Meeting on Optical Amplifiers and Applications, Santa Fe, NM, 1992, PD-1; T. Kitagawa, K. Hattori, K. Shuto, M. Yasu, M. Kobayashi, and. M. Horiguchi, Electron. Lett. **28**, 1818 (1992).

[8] K. Shuto, K. Hattori, T. Kitagawa, and M. Horiguchi, Proc. 19th Europ. Conf. on Opt. Comm., Montreux, Switserland, 1993, 53.

[9] T. Feuchter, E. K. Mwarania, J. Wang, L. Reekie, and J. S. Williams, IEEE Phot. Techn. Letts. **4**, 542 (1991).

[10] P. Becker, R. Brinkmann, M. Dinand, W. Sohler, and H. Suche, Appl. Phys. Lett. **61**, 1257 (1992).

[11] G. N. van den Hoven, R. J. I. M. Koper, A. Polman, C. van Dam, J. w. M. van Uffelen, and M. K. Smit, Appl. Phys. Lett. **68**, 1886 (1996).

[12] Norwood *et al*, B. Booth, in *Polymers for Lightwave and Integrated Optics*, edited by L.A. Hornak, Dekker, New York (1992).

[13] G. Stein, and E. Würzberg, J. Chem. Phys. **62**, 208 (1975).

[14] J. L. Kropp, and M. W. Windsor, J. Chem. Phys. **42**, 1599 (1965).

[15] M. P. Oude Wolbers, F. C. J. M. van Veggel, B. H. M. Snellink-Ruël, J. W. Hofstraat, A. J. Geurts, and D. N. Reinhoudt, submitted to J. Am. Chem. Soc.

[16] C. F. Born, D. R. Hüffner, in *Absorption and Scattering of Light by Small Particles*, Wiley, New York (1983).

[17] A. Polman, D. C. Jacobson, D. J. Eaglesham, R. C. Kistler, and J. M. Poate, J. Appl. Phys **70**, 3778 (1991).

[18] E. Snoeks, G. N. van den Hoven, and A. Polman, J. Appl. Phys. **73**, 8179 (1993).

[19] G. N. van den Hoven, E. Snoeks, A. Polman, J. M. W. van Uffelen, Y. S. Oei, M. K. Smit, Appl Phys. Lett. **62**, 3065 (1993).

[20] J. N. Sandoe, P. H. Sarkies, and S. Parke, J. Phys. D: Apppl. Phys. **5**, 1788 (1972).

[21] W. J. Miniscalco, J. Lightwave Techn. **9**, 234 (1991).

[22] G. N. van den Hoven, E. Snoeks, J. A. van der Elsken, C. van Dam, J. W. M. van Uffelen, M. K. Smit, Appl. Opt. in press (1996).

[23] W. J. Miniscalco, R. S. Quimby, Opt. Lett. **16**, 258 (1991).

[24] G. N. van den Hoven, E. Snoeks, A. Polman, C. van Dam, J. W. M. van Uffelen, and M. K. Smit, J. Appl. Phys. **79**, 1258 (1996).

Part II Light emitting diodes based on erbium-implanted hydrogenated amorphous silicon

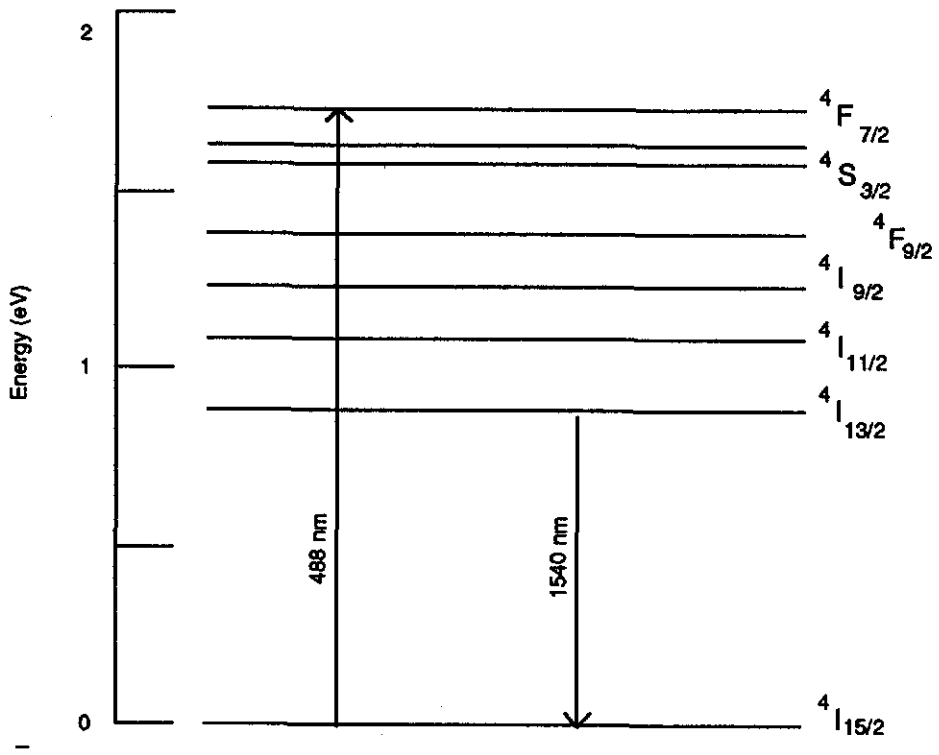

Fig. 1. Schematic energy diagram of the free Er^{3+} ion. Shown are the excitation band $^4F_{7/2}$ and the transition from the first excited state $^4I_{13/2}$ to the ground state $^4I_{15/2}$.

1 Introduction

Doping of silicon with erbium has become a major field of research because of its possible applications in silicon-based opto-electronics [1-9]. In its trivalent state, the rare-earth erbium (Er) has a 4f shell which is only partly filled. This 4f shell is shielded from its surroundings by filled outer electron shells, resulting in relative sharp intra 4f transitions. The transition between the 4f levels $^4I_{13/2}$ and $^4I_{15/2}$ is of particular interest, because its wavelength of 1.5 μm (see figure 1) coincides with the window of maximum transmission for silica optical fibers.

Ennen *et al.* [1, 2] showed photoluminescence (PL) and electroluminescence (EL) of Er^{3+} in crystalline Si at 77 K. However upon increasing the temperature the luminescence intensity decreases due to a strong temperature quenching and no PL and EL were seen at room temperature. Recently it has been observed that co-doping of crystalline Si (c-Si) with C and O at concentrations of 10^{20} /cm^3 enhances the PL yield [3-5] and room temperature EL at 1.54 μm has been observed [6,7]. Amorphous silicon (a-Si) is also an interesting host for Er. Due to the amorphous structure of the material more Er and more impurities can be incorporated compared to c-Si. Er doped pure a-Si shows luminescence only at low temperature (77K) [8], but room temperature PL [9] and EL [10] have been observed for heavily oxygen-doped (30 at.%) a-Si (SIPOS). However the electrical properties of SIPOS are rather poor. Hydrogenated amorphous silicon (a-Si:H) has a much better electrical quality than SIPOS. In fact a-Si:H is the base material for a-Si solar cells, which show rather good efficiencies. Recently room temperature PL of Er implanted a-Si:H has been observed and an increase in PL intensity was seen upon co-doping with 1.0 at.% O [11].

In the present report the co-doping with O is further investigated and Er implanted a-Si:H p-i-n diodes are made, and show room temperature EL at 1.5 μm.

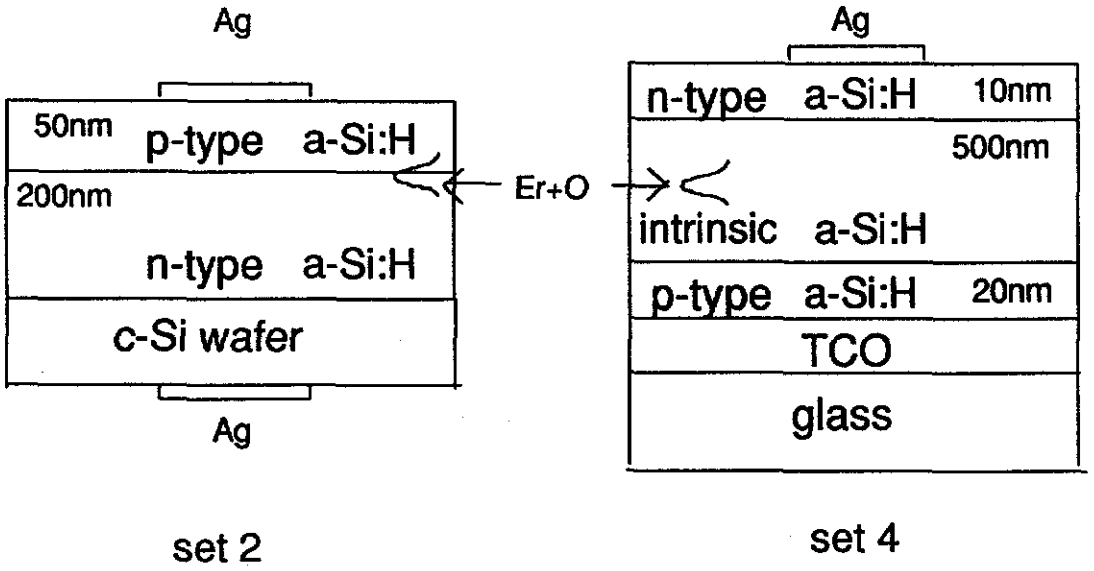

Fig.2. Diode structures as used for PL and EL measurements

set	1a	1b	2	3	4a	4b
substrate	c-Si (100) Cz	c-Si (100) Cz	c-Si (100) Cz	Corning glass	glass/TCO	glass/TCO
structure	n	n	n-p	i	p-i-n	p-i-n
thickness (nm)	200	200	200-50	500	20-500-10	20-500-10
Er fluence (10^{14} cm^{-2})	5	5	5	5	5	5
impl. energy (keV)	250	250	125	700	700	700
O impl. energy (keV)		30	50	80	80	80
fluences (10^{14} cm^{-2})		8, 16, 24	20	32	32	32
O impl. energy (keV)		50		120	120	120
fluences (10^{14} cm^{-2})		1.5, 3, 4.5		55	55	55
O concentration (at.%)		0.5, 1.0, 1.5	1.0	1.0	1.0	1.0
anneal temp. (°C)	200, 300, 400, 500	300	300	100, 200, 300, 400, 500	400	200,300

Table 1: Sample preparation parameters of all deposited a-Si:H sets.

2 Experimental

Four sets of depositions were made. Hydrogenated amorphous silicon (a-Si:H) layers were deposited by Plasma Enhanced Chemical Vapour Deposition (PECVD) of SiH_4. First, a 200 nm thick phosphorous doped (n-type) a-Si:H layer was deposited on a Czochralski grown (Cz) (100) crystalline silicon (c-Si) wafer (set 1). Second, a diode set was made, consisting of a 50 nm thick boron doped (p-type) a-Si:H layer on top of a 200 nm thick n-type a-Si:H layer on a CZ-Si wafer (set 2). Third, a 500 nm thick intrinsic a-Si:H layer (i - a-Si:H) was deposited on Corning glass (set 3). Fourth, two sets of a p-i-n diode structure were deposited on barium borosilicate glass with a transparent conductive oxide (TCO) in between (set 4a and 4b). The diode structures of sets 2 and 4 are given in figure 2.

All sets were implanted with erbium (Er) at a fluence of $5*10^{14}$ cm^{-2}. In the sets with one single layer (set 1 and 3), the implantation energy was chosen such that the peak Er concentration lies in the middle of the layer. In set 2 the implantation energy of 125 keV results in a maximum Er concentration near the n-p junction and for set 4 the Er is positioned near the middle of the intrinsic layer. The energies used are given in table 1.
Set 1 consists of two sub sets; set 1a which was not co-doped with O and set 1b which was co-doped with 30 keV and 50 keV O, resulting in an almost homogenous O concentration in the Er-doped region. Three different O concentrations were implanted: 0.5 at.%, 1.0 at.% and 1.5 at.%. All other sets were co-doped with 1.0 at.% O. The used O implantation energies and fluences are given in table 1.

Post implantation anneals at temperatures ranging from 100 °C to 500 °C for 30 minutes were performed on all sets. The used temperatures for each set are given in table 1.

After annealing Ag front contacts were made on the two diode sets (sets 2 and 4) by evaporation of Ag through a contact mask. The back contact of the p-i-n diode (set 4) was made by evaporating two Ag side contacts on top of the TCO layer before the a-Si:H was deposited. Two planar Ag contacts were evaporated on the intrinsic a-Si:H (set 3) for conductivity measurements.

Rutherford Backscattering Spectroscopy measurements (RBS) were carried out using 2.0 MeV He^+ and a scattering angle of 130° or 135°.

Photoluminescence (PL) measurements were performed using the 515 nm line of an Ar ion laser at different powers. The laser beam was modulated with a mechanical chopper at a frequency of 30 Hz or an acousto optic modulator at a frequency of 20 Hz. The samples were mounted in a closed-cycle helium cryostat, enabling measurements at temperatures ranging from 12 K to room temperature. The PL signal was focused into a monochromator and detected with a liquid-nitrogen-cooled Ge detector, using standard lock-in techniques. The spectral resolution was 6 nm. Lifetime measurements were performed by monitoring the luminescence decay after switching off the pump beam using the acousto-optic modulator. The time resolution of the system was 30 μs.

Electroluminescence (EL) measurements were performed by applying a blocked voltage pulse to the contacts of the diode. Voltage, current and EL signal were monitored in the same set-up as for PL. The EL signal of the p-n diode (set 2) was collected from the side of the sample and of p-i-n diode (set 4) through the TCO and the glass.

Current-Voltage (I-V) characteristics were measured at room temperature with an Oriel Solar Simulator set-up under dark conditions.

In order to know if the incorporation of Er and O leads to a donor or acceptor behaviour in a-Si:H, the conductivity of Er and O implanted intrinsic a-Si:H was measured in a vacuum system by measuring the current and applied voltage as a function of temperature between room temperature and 325 K. According to Mott and Davids [12, 13], the temperature dependence of the conductivity σ for electrons is assumed to be given by :

$$\sigma = \sigma_0 e^{-\frac{E_{act}}{kT}} \qquad (1)$$

Where E_{act} is the energy difference between the lower edge of the conduction band and the Fermi level. In intrinsic a-Si:H the Fermi level lies midgap, resulting in $E_{act} \approx 0.8$ eV for intrinsic a-Si:H.

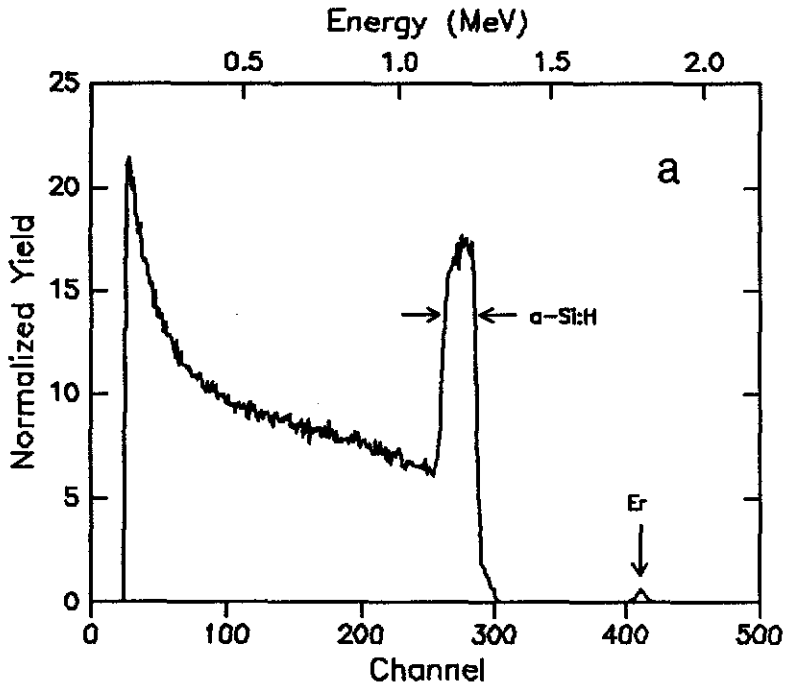

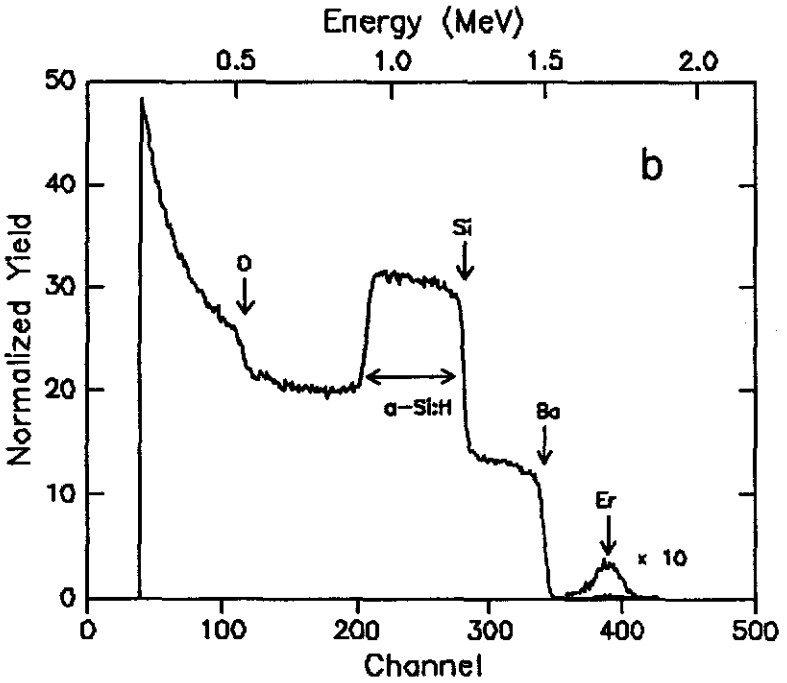

Fig.3. RBS Spectra for a) an Er implanted ($5*10^{14}$ Er/cm^2; 125 keV) p-n diode on c-Si and b) an Er implanted ($5*10^{14}$ Er/cm^2; 700 keV) p-i-n diode on TCO and glass. A 2 MeV He beam was used at a scattering angle of 130° (a) and 135° (b). In (b), the Er signal was multiplied by a factor 10.

3. Results and discussion

3.1 Rutherford Backscattering Spectrometry

The result of Rutherford Backscattering measurements (RBS) are shown in figure 3. Figure 3(a) shows a channelling RBS spectrum of the a-Si:H p-n diode structure on c-Si (set 2). A region with high yield is seen between channels 250 and 280, and corresponds to the amorphous layer. The a-Si:H thickness is 210 nm. The small signal above channel 400 is a result of the implanted Er. It corresponds to $5*10^{14}$ atoms/cm^2 Er and the Er depth profile peaks at a depth of 100 nm with a full width at half maximum (FWHM) of 70 nm. A random RBS spectrum of the p-i-n diode structure (set 4) is seen in figure 3(b). The high yield region between channel 210 and 280 arises from the a-Si:H, and is superimposed on a background due to Ba from the glass substrate. The Ba and O edges, shifted to account for the a-Si:H surface layer, are also shown. Again the a-Si:H layer thickness can be deduced from the spectrum and this results in a thickness of 650 nm.. The small signal below channel 400 corresponds to the implanted Er and corresponds to $5*10^{14}$ Er/cm^2 . The Er depth profile peaks at a depth of 275 nm with a FWHM of 165 nm. The Er is thus positioned near the middle of the intrinsic layer. The composition of the glass as deduced from a fit through the measurement is: Si 24 at.%, B 24 at.%, Ba 3 at.% and O 48 at.%.

3.2 Photoluminescence excitation and emission spectroscopy

Room temperature PL spectra of Er implanted a-Si:H are shown in figure 4. Figure 4(a) shows the PL spectra of n-type a-Si:H on c-Si (set 1) co-doped with 0 at.%, 0.5 at.%, 1.0 at.%, and 1.5 at.% O, measured at a pump power of 150 mW. The small peak around 1.54 μm for the 0.5 and 1.0 at.% samples, is due to the intra 4f transition from the first excited to the ground state of the Er^{3+} ion state (see figure 1). The PL intensities are very weak. The sample co-doped with 1.5 at.% O and the one without O co-doping, show no measurable Er-related PL. Figure 4(b) shows the PL spectra of intrinsic a-Si:H on Corning glass (set 3), at a pump power of 40 mW, and the p-i-n diode structure on TCO and glass (set 4b), at a pump power of 30 mW, both annealed at 300 °C. These samples show clear room temperature PL due to Er^{3+}.

From figure 4(a) it can be concluded that co-doping with 1.0 at.% O results in the highest room temperature PL intensity of these samples. This concentration was chosen for the co-doping of later sets.

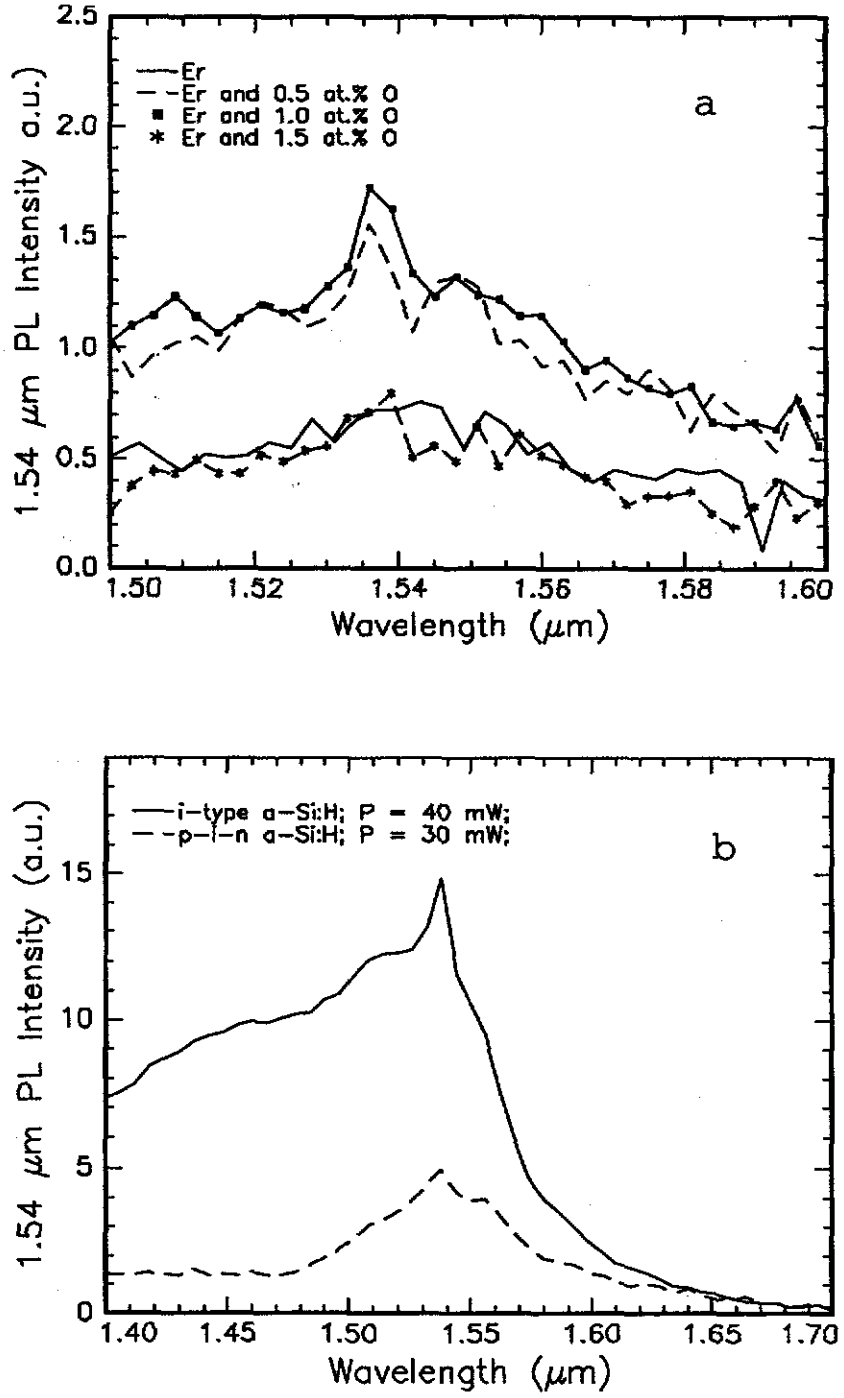

Fig.4. Room temperature PL spectra of (a) an Er implanted ($5*10^{14}$ Er/cm^2; 125 keV) p-n diode, co-doped with 0.5 at.% O and 1.0 at.% O (set 1b), and (b) of Er implanted ($5*10^{14}$ Er/cm^2; 700 keV) intrinsic a-Si:H (set 3) at a pump power of 40 mW and a p-i-n a-Si:H diode (set 4a) at a pump power of 30 mW, all annealed at 300 °C .

Figure 5 shows the PL excitation spectrum at 12 K of Er implanted n-type a-Si:H (set 1) annealed at 300 °C for 30 minutes. The PL intensity at 1.54 μm is measured for different wavelengths: 476.5 nm, 588 nm, 496.5 nm, 501.4 nm, 501.4 nm and 514.5 nm, at a constant pump power of 150 mW.

The PL intensity slightly increases as a function of the excitation wavelength, but shows no peaks near the wavelengths of Er absorption bands (488 nm and 514.5 nm). This indicates that the Er is not optically excited like e.g. the organic Er^{3+}-complexes (see figure 5 in chapter I of this thesis), but electrically excited. This is thought to occur via an electron-hole pair mediated process [5], which is schematically indicated in figure 6. First, a laser induced electron-hole pair is trapped at an Er-related defect level in the Si bandgap (T). Then the recombination energy of the electron-hole pair is transferred to the Er^{3+} ion (E) and excites the Er. At high temperatures, the luminescence can be quenched by de-excitation of the Er^{3+} ion followed by backtransfer (B) of the energy to the Si crystal electronic system (e.g. the generation of a trapped electron), or by de-trapping of the trapped electron-hole pair (D).

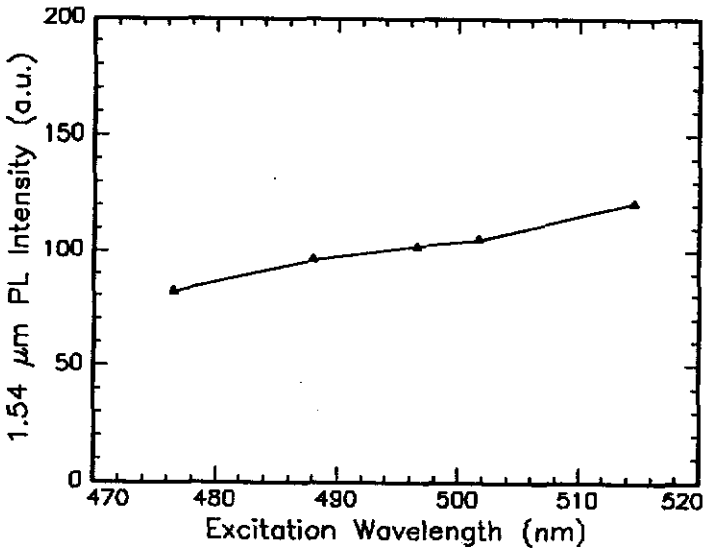

Fig. 5. PL excitation spectrum of Er implanted a-Si:H (set 1a). The 1.54 μm Er^{3+} emission is measured as function of excitation wavelength at a constant pump power of 150 mW.

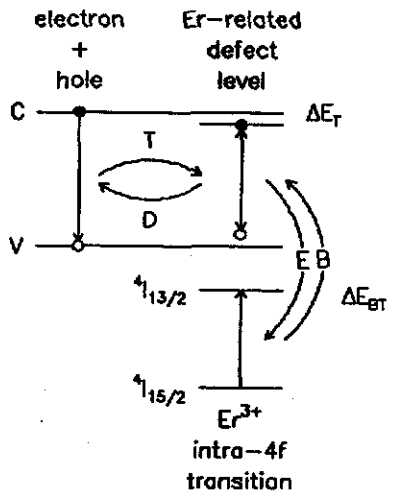

Fig. 6. Schematic representation of the excitation mechanism of Er in Si.

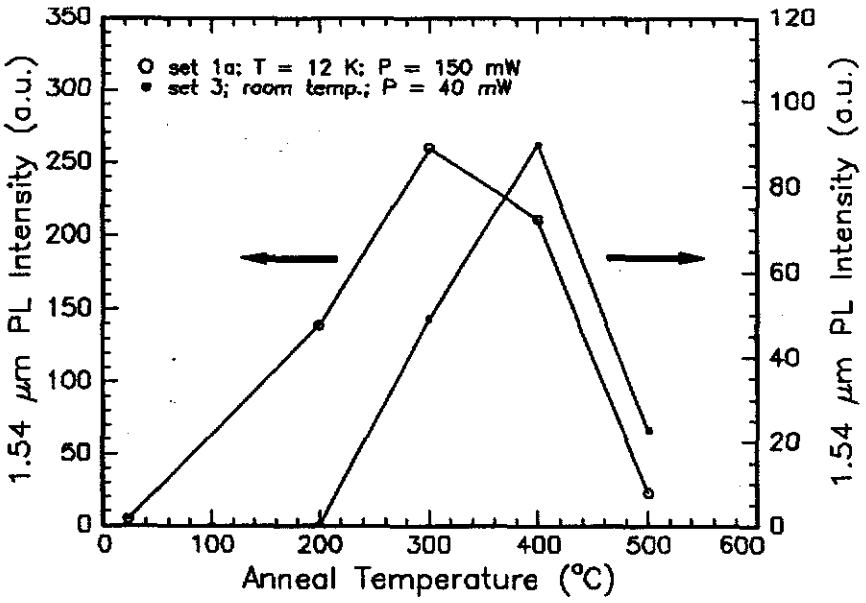

Fig.7. 1.54 μm PL intensity as a function of anneal temperature for n-type a-Si:H on c-Si (set 1a), measured at 12 K (left axis) and intrinsic a-Si:H on glass (set 3), measured at room temperature (right axis).

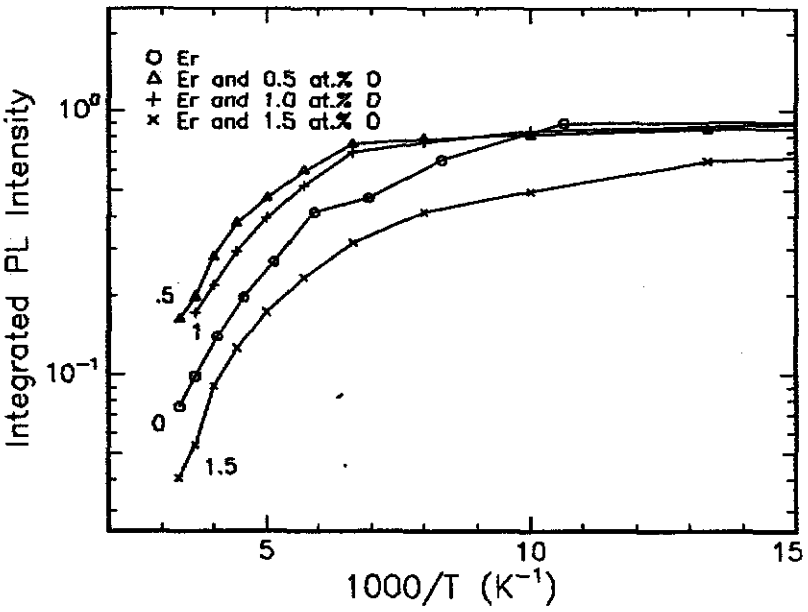

Fig. 8. Arrhenius plot of the integrated 1.54 μm PL intensity of Er implanted a-Si:H (with and without O co-doping at 0.5, 1.0, and 1.5 at.%, set 1), measured at a wavelength of 514.5 nm and a pump power of 150 mW.

3.3 Annealing of a-S:H and temperature quenching

The 1.54 μm PL intensity as a function of anneal temperature is shown in figure 7. Data are shown for n-type a-Si:H on c-Si (set 1a) at 12 K and a pump power of 150 mW and for intrinsic a-Si:H on Corning glass (set 3) at a pump power of 40 mW at room temperature. The PL intensity increases with temperature till 300-400 °C and decreases at higher temperatures. The samples on c-Si annealed at temperatures above 250 °C showed circularly shaped spots, which are thought to arise from H bubbles due to the diffusion of H out of the a-Si:H, together with a bad sticking of the a-Si:H on the c-Si substrate. The sticking of a-Si:H on glass is better (this is known form research on a-Si:H solar cells), so a glass substrate was chosen for the p-i-n diode set (set 4) in order to reduce the bubbles from annealing.

Until 300 °C anneal , no bubbles were observed for these p-i-n diodes on glass. At 400 °C , however, this set showed the same bubbles as the samples on a c-Si substrate. The increase in the PL intensity up to anneal temperatures of 300-400 °C is attributed to annealing of implantation induced defects. It is known that at these anneal temperatures the H is mobile enough to passivate electrical defects [14]. As defects can quench the luminescence, annealing will result in an increase in PL intensity. Above 400 °C the H becomes so mobile that it diffuses out of the sample resulting in a decrease in the PL intensity.

Figure 8 shows the temperature quenching of the PL intensity of n-type a-Si:H on a c-Si substrate, co-doped with different O concentrations and annealed at 300 °C for 30 minutes (set 1). All data are normalised to the integrated PL intensity at 12 K. The pump power was 150 mW. The undoped sample shows a temperature quenching from 12 to 300 K of a factor 12. The co-doping of 0.5 at.%, 1.0 at.% and 1.5 at.% O results in quenching by a factor of 6, 5, and 25 respectively.

The co-doping of O reduces the temperature quenching up to a doping concentration of about 1.0 at.%. This is also seen for Er and O doped c-Si, where co-doping of O has been shown to improve the room temperature Er luminescence, due to an increase in the optically active fraction of Er ions and a reduction in temperature quenching (see ref.[5]). Above an O concentration of 1.0 at.% the temperature quenching strongly increases. It may be that the presence of too much O reduces the carrier lifetime in a-Si:H, and as a result increases the temperature quenching [5].

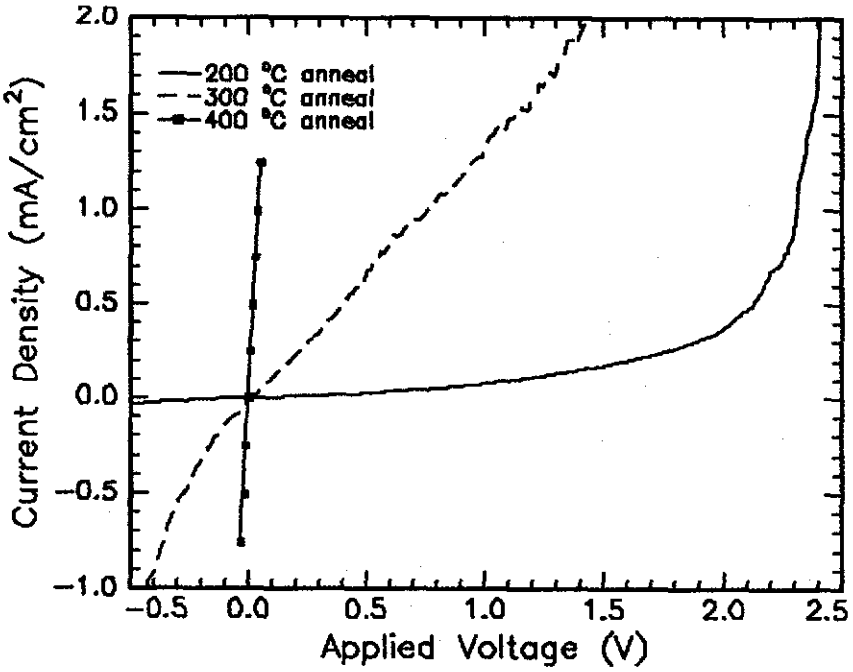

Fig. 9. J-V curves of Er-implanted a-Si:H p-i-n diode structures on glass (set 4) for three different anneal temperatures: 200, 300 and 400 °C.

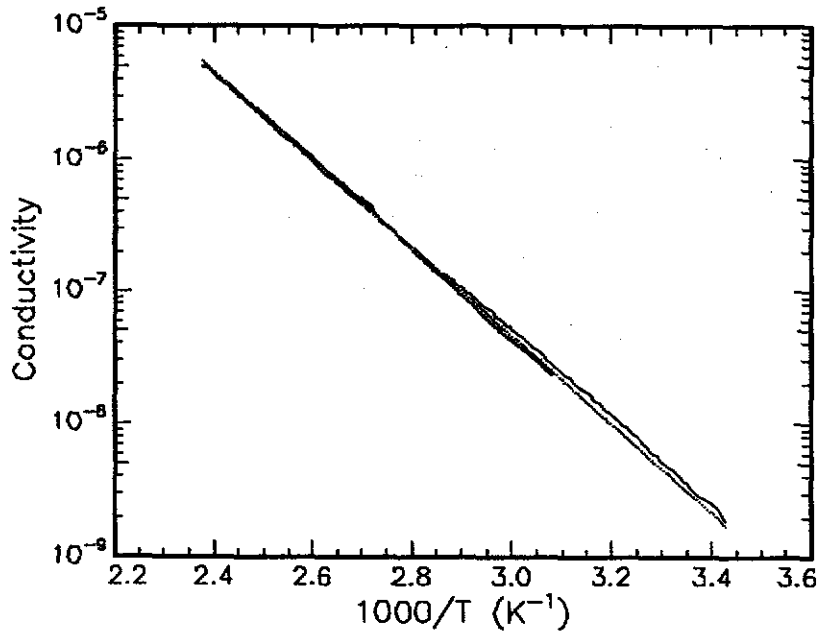

Fig. 10. Arrhenius plot of the conductivity of Er and O implanted intrinsic a-Si:H (set 3). A linear fit through the data results in an activation energy of 0.66 eV.

3.4 J-V and conductivity measurements

Figure 9 shows the current density (J) as a function of the applied voltage for the Er-implanted p-i-n diode set (set 4). The sample annealed at 200 °C shows clear diode characteristics. The samples annealed at 300 °C and 400 °C show a nearly linear dependence on the applied voltage, not characteristic for a diode.

These bad diode characteristics are attributed to the fact that the 300-400 °C anneal temperatures make diffusion of the dopant of the p-type a-Si:H (boron) into the intrinsic a-Si:H region possible. At lower anneal temperatures, the diode structure looks still in tact.

Figure 10 shows a conductivity measurement of Er and O implanted intrinsic a-Si:H on Corning glass (set 3). A fit of equation (1) through the data results in an activation energy of 0.66±0.01 eV.

In intrinsic materials the Fermi level lies midgap. For a-Si:H, which has a bandgap of 1.6 eV, this means that the activation energy would be 0.8 eV. The Fermi level of Er and O implanted a-Si:H is thus slightly shifted upwards resulting in light n-type material. This should be taken into account when designing optimised diode structures.

3.5 Electroluminescence spectroscopy

Electroluminescence (EL) measurements were performed on the p-i-n (set 4) and p-n (set 2) diode structures. Figure 10 shows the room temperature EL spectrum of the p-i-n diode structure on TCO and glass annealed at 400 °C under forward bias (set 4a). In this case the positive voltage is connected to the contact at the p-type a-Si:H side and the negative voltage is connected to the contact at the n-type side. The applied forward voltage is 4.45 V at a current of 19 mA. A clear Er^{3+} luminescence peak is seen at 1.53 μm, superimposed on a broad background which is attributed to defect luminescence from a-Si:H. Also shown is the PL spectrum of the same sample at a pump power of 40 mW.
The samples annealed at 200 °C and 300 °C showed broad room temperature EL spectra, without the characteristic peak for Er^{3+} at 1.53 μm. No EL was observed for the Er-implanted p-n diodes of set 2, which was deposited on a Si substrate. This was attributed to the large density of bubbles in samples after annealing.

The maximum in luminescence intensity for a 400 °C anneal is also seen in the PL measurements of figure 7. This was attributed to incomplete annealing of implantation induced defects for anneal temperatures of 200-300 °C. The data in sections 3.3-3.5 indicate that on the one hand high anneal temperatures (400 °C) are required to optimise the Er^{3+} PL intensity, while good diode behaviour of the p-i-n junctions is only observed for low anneal temperatures (200 °C). At this stage, the optimum EL is found after 400 °C annealing. It is expected that better EL signals can be obtained from a-Si:H diodes which are doped with Er in the PECVD process. In this case, the defects due to the Er implantation process can be avoided, and lower anneal temperatures may be needed to activate the Er.

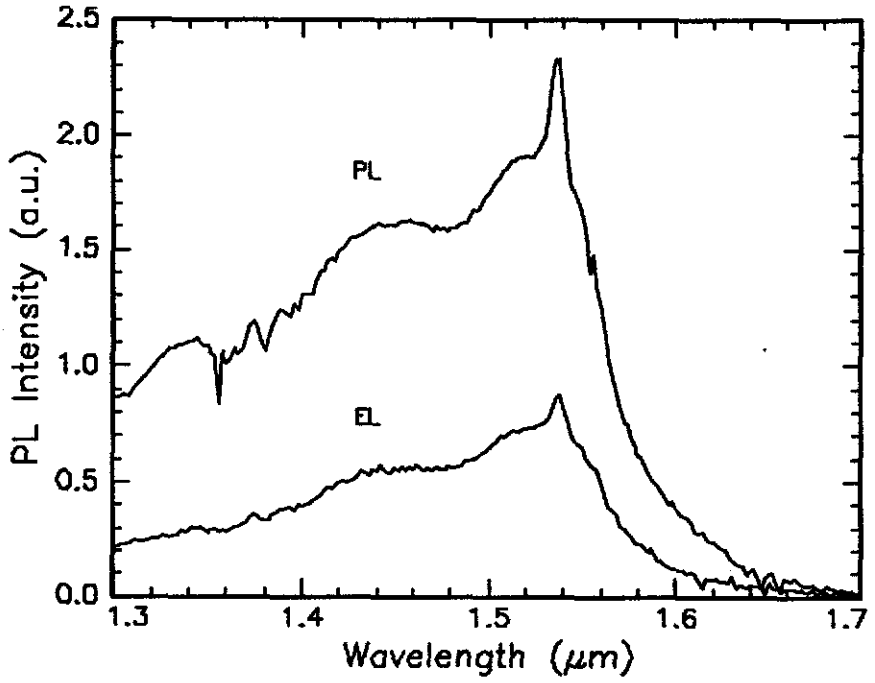

Fig. 11. EL and PL spectrum of Er implanted a-Si: H p-i-n diode, co-doped with 1.0 at.% O annealed at 400 °C for 30 minutes (set 4a); EL: V = 4.45V I = 19 mA; PL: P = 40 mW, monochromator slits half as wide as with EL.

4 Conclusions

Er-implanted intrinsic a-Si:H and a-Si:H p-i-n diode films show photoluminescence at 1.54 μm. Films without O co-implantation show a temperature quenching between 15-300 K by a factor 12. The quenching can be reduced by co-implanting 0.5 or 1.0 at.% O. Higher O concentrations increase the quenching, presumably due to a effect on the minority carrier lifetime.

Room temperature electroluminescence from Er^{3+} at 1.53 μm is seen for Er implanted p-i-n a-Si:H diodes on a TCO covered glass substrate, co-doped with 1.0 at.% O. A high anneal temperature (400 °C) is needed for defect annealing, but deteriorates the electrical characteristics of the diode. Optimum electroluminescence is found for an anneal of 400 °C.

Photoluminescence excitation measurements show that Er in a-Si:H is electrically excited, via an electron-hole pair mediated process. This is also indicated by the dependence of the PL intensity on the annealing temperature, which shows a maximum at annealing temperatures of 300-400 °C. The increase for anneal temperatures up to 300-400 °C is due to annealing of implantation induced defects. Above 300-400 °C the PL intensity decreases, presumably as a result of outdiffussion of H.

Improvements can be made by optimisation of the diode structure and material. The defects due to the Er-implantation process can be avoided if the Er can be incorporated during the a-Si:H deposition process, and lower anneal temperatures can be used.

5 References

[1] H. Ennen, J. Schneider, G. Pomrenke, and A. Axmann, Appl. Phys. Lett. **43**, 943 (1983).

[2] H. Ennen, G. Pomrenke, A. Axmann, K. Eisele, W. Haydl, and J. Schneider, Appl. Phys. Lett. **46**, 381 (1985).

[3] J. Michel, J.L. Benton, R. F. Ferrante, D. C. Jacobson. D. J. Eaglesham, E. A. Fitzgerald, Y. H. Xie, J. M. Poste, and L. C. Kimerling, J. Appl. Phys. **79**, 2672 (1991).

[4] S. Coffa, G. Franzò, F. Priolo, A. Polman, and R. Serna, Phys. Rev. B **49**, 16313 (1994).

[5] F. Priolo, G. Franzò, S. Coffa, A. Polman, S. Libertino, R. Barklie, and D. Carey, J. Appl. Phys. **78**, 3874 (1995).

[6] G. Franzò, F. Priolo, S. Coffa, A. Polman, and A. Carnera, Appl. Phys. Lett. **64**, 2235 (1994).

[7] B. Zheng, J. Michel, F. Y. G. Ren, L. C. Kimberling, D. C. Jacobson, and J. M. Poate, Appl. Phys. Lett. **64**, 2842 (1994).

[8] J. S. Custer, E. Snoeks, and A. Polman, Mater. Res. Soc. Proc. **235**, 51 (1992).

[9] G. N. van den Hoven, Jung. H. Shin, A. Polman, S. Lombardo, and S. U. Campisano, J. Appl Phys. **78**, 2642 (1995).

[10] S. Lombardo, S. U. Campisano, G. N. van den Hoven, and A. Polman, J. Appl. Phys. **77**, 6504 (1995).

[11] Jung H. Shin, R. Serna, G. N. van den Hoven, A. Polman, W. G. J. H. M. van Sark, and A. M. Vredenberg, Appl. Phys. Lett. **68**, 46 (1996).

[12] N. F. Mott and E. A. Davis, *Electronic Processes in Non-Crystalline Materials*, 2nd ed., University Press, Oxford (1979).

[13] N. F. Mott, Chapter 4 in *The physics of Hydrogenated Amorphous Silicon II*, J. D. Joannopoulos and G. Lucovsky, editors, Springer-Verlag, Berlin, Heidelberg, New York, Tokyo, 169 (1979).

[14] P. A. Stolk, A. J. M. Berntsen, F. W. Saris, and W. F. van der Weg, Mat. Res. Soc. Symp. Proc. **297**, 127 (1993).

Dankwoord

Alleen dankzij de medewerking van collega's, familie en vrienden heb ik mijn afstudeeronderzoek op deze wijze kunnen voltooien. Hun hulp en steun in het afgelopen jaar hebben mijn onderzoek gemaakt tot dat wat het nu is. Met name wil ik hier Albert Polman, mijn begeleider, heel hartelijk bedanken voor alle tijd die hij in mijn onderzoek heeft gestoken. Albert wist door zijn heldere, positieve kijk op de zaken, toch altijd weer een lichtpuntje naar voren te halen en mij weerte inspireren om verder te gaan. Pieter Kik, Mark Brongersma en Gerlas van den Hoven, de (ex)OIO's uit de groep en Michiel de Dood, de ander student, allemaal bedankt voor de (on)zinnige discussies en hulp in experimentele noodgevallen. Zonder jullie 'magic hands' had mijn afstudeeronderzoek veel langer geduurd. Ook Hans Hofstraat, Manon Oude Wolbers, Frank van Veggel, Wilfried van Sark en Remco van der Heijden wil ik bedanken voor het maken van de samples en de nuttige tips. Verder natuurlijk alle andere die op welke wijze dan ook geholpen hebben dit onderzoek tot een goed einde te brengen, bedankt !

Als laatste wil ik mijn familie bedanken. Vooral mijn ouders die ervoor hebben gezorgd dat ik al mijn aandacht aan mijn studie kon wijden. Steven, Nynke, Carola en sinds kort ook Roel, die voor de nodige afleiding hebben gezorgd. Ronald voor zijn altijd aanwezige interesse in mijn bezigheden. En tot slot Léon die de afgelopen maanden de laatste loodjes heeft helpen verlichtten.
Bedankt !